Supplementary Information (SI) for Journal of Materials Chemistry A.
This journal is © The Royal Society of Chemistry 2024

Supplementary Materials for

"Electrolyte Engineering for the Mass Exfoliation of Graphene Oxide across Wide Oxidation Degrees"

Authors: Huili Ren[a]†, Xiaopei Xia[a]†, Yingzhi Sun[a], Yi Zhai[a], Zongzheng Zhang[b], Jiahao Wu,[a] Jing Li[a*], Mingjie Liu[a]

Address:

[a] Key Laboratory of Bio-inspired Smart Interfacial Science and Technology of Ministry of Education, School of Chemistry, Beihang University, Beijing 100191, China.

[b] School of Chemistry and Materials Science, Ludong University, Yantai 264025, China.

E-mail: chmlij@buaa.edu.cn

† These authors contributed equally to this work.

This Supplementary Information includes the following sections:

Table 2. The elemental ratios of carbon to oxygen (C/O) of various types of graphene and their respective oxidants, along with the oxidation duration.

Experimental Section/Methods

Materials： Graphite foil (width: 10 cm, thickness: 0.05 mm, purity: 98%) was purchased from SKF (Tianjin) Energy Saving Technology Co., Ltd. Hydrazine sulfate, ammonium sulfate, acrylamide, N,N'-methylenebis(2-propenamide), ammonium persulfate, N,N,N',N'-tetramethylethylenediamine, calcium chloride ($CaCl_2$) and sodium alginate (SA) were purchased from Aladdin and used without any additional purification. Polyvinyl alcohol (PVA) was purchased from Sigma-Aldrich and used without further purification. Concentrated sulfuric acid (purity: 95% ~ 98%) was purchased from Jing Chun Chemical Co. Ltd and used without further purification.

Electrochemical exfoliation of GO across wide oxidation degrees

Commercial graphite foils served as the anode (with platinum mesh as the cathode) and were pre-intercalated with concentrated sulfuric acid in an electrochemical cell at a voltage of 2.2 V. Subsequently, the pre-intercalated graphite was transferred to the second cell for exfoliation/oxidation at a voltage of 10 V, containing various electrolytes (hydrazine sulfate: 0.01 M, 0.05 M, 0.1 M, 0.2 M; H_2SO_4: 10 wt%, 30 wt%, 50 wt%, 70 wt%; 50 wt% H_2SO_4 mixed with 0.1 M ammonium sulfate, 0.0001 M $KMnO_4$, 0.001 M $KMnO_4$, 0.01 M $KMnO_4$, and 0.1 M $KMnO_4$). It is important to note that EcE-G1 denotes the electrolyte solution composed of 50% H_2SO_4-0.01 M hydrazine sulfate used in the second stage. Similarly, EcE-G2, EcE-G3, EcE-G4, EcE-G5, and EcE-G6 represent the electrolyte solutions composed of 50% H_2SO_4-0.1 M hydrazine sulfate, 50% H_2SO_4-0.001 M $KMnO_4$, 50% H_2SO_4-0.0001 M $KMnO_4$, 50% H_2SO_4-0.01 M $KMnO_4$, and 50% H_2SO_4-0.1 M $KMnO_4$, respectively.

Table S1. The diagram of correspondence between sample labels and electrolyte compositions in the second exfoliation step.

Types of graphene	Oxidant
EcE-G1	0.01 M Hydrazine sulfate
EcE-G2	0.1 M Ammonium sulfate
EcE-G3	50 wt% H_2SO_4 + 0.001 M $KMnO_4$
EcE-G4	50 wt% H_2SO_4 + 0.0001 M $KMnO_4$
EcE-G5	50 wt% H_2SO_4 + 0.01 M $KMnO_4$
EcE-G6	50 wt% H_2SO_4 + 0.1 M $KMnO_4$

Preparation of polyacrylamide (PAAm) hydrogels

A uniform solution phase was prepared by dissolving 15 g of acrylamide, 0.3 g of N,N′-methylenebis(acrylamide), and 0.3 g of ammonium persulphate in 100 mL of distilled water. Subsequently, 300 μL N,N,N',N'-tetramethylethylenediamine was added to initiate radical polymerization for 5 minutes at room temperature. The obtained hydrogels were then thoroughly rinsed with abundant water to remove unreacted components and ensure the complete swelling of the hydrogels.

Fabrication of GO-based composite films

Before the fabrication process, the PAAm hydrogels were soaked in deionized water to achieve full swelling. Subsequently, $CaCl_2$ power was added to the mixture to form a 0.05 M $CaCl_2$ solution, facilitating further impregnation of Ca^{2+} into the PAAm hydrogels. Additionally, a solution containing PVA, SA, GO, and water was sequentially prepared by sequential addition into a beaker and stirred until homogeneous, with a mass ratio of SA : PVA : GO = 5 : 4 : 1 (referred to as the SA-based solution). During fabrication, an appropriate amount of the SA-based solution was poured onto the

PAAm hydrogel-oil interface. Notably, due to superspreading and the diffusion of Ca^{2+} ions from the PAAm hydrogel surface, which facilitated the crosslinking of SA, the SA-based solution rapidly spread between the oil and PAAm hydrogel interface, forming a stable and homogeneous liquid layer. This layer was eventually transformed into a uniform hydrogel film, easily separated from the PAAm hydrogel surface in a water bath. Following this, the composite gel films were dried in an oven at 60 °C and atmospheric pressure for 5 hours, resulting in the collection of uniform and continuous GO-based composite films.

Characterizations

High-resolution transmission electron microscopy (HRTEM) was conducted using an FEI Titan 80–300 S. Raman spectra were acquired utilizing a LabRAM HR Evolution with a 532 nm laser at ambient conditions. X-ray diffraction (XRD) patterns were collected on Brucker D8 DISCOVER (Cu Kα radiation, λ = 1.54056 Å) at room temperature, with diffraction patterns measured in a 2θ range of 8-70° at a step speed of 5°/min. X-ray photoelectron spectroscopy (XPS) measurements were conducted with ESCALABXi+ under ultrahigh vacuum conditions. Small-angle X-ray scattering (SAXS) measurements were carried out at Xeuss 3.0 HR using an incident Cu-Kα X-ray beam, oriented vertically to the sample plane, with a detector-sample distance of 55 mm. Thermogravimetric analysis (TGA) results were obtained using the STA 449 F5 Jupiter instrument, with a temperature range between room temperature and 800 °C under a nitrogen (N_2) atmosphere. Atomic force microscopy (AFM) images were obtained in tapping mode using a Bruker Dimension Icon. Mechanical properties were assessed using the ESM303 instrument at a tensile rate of 0.5 mm/min. UV-vis absorption spectra were measured using the SHIMADZU UV-3600 Plus spectrophotometer.

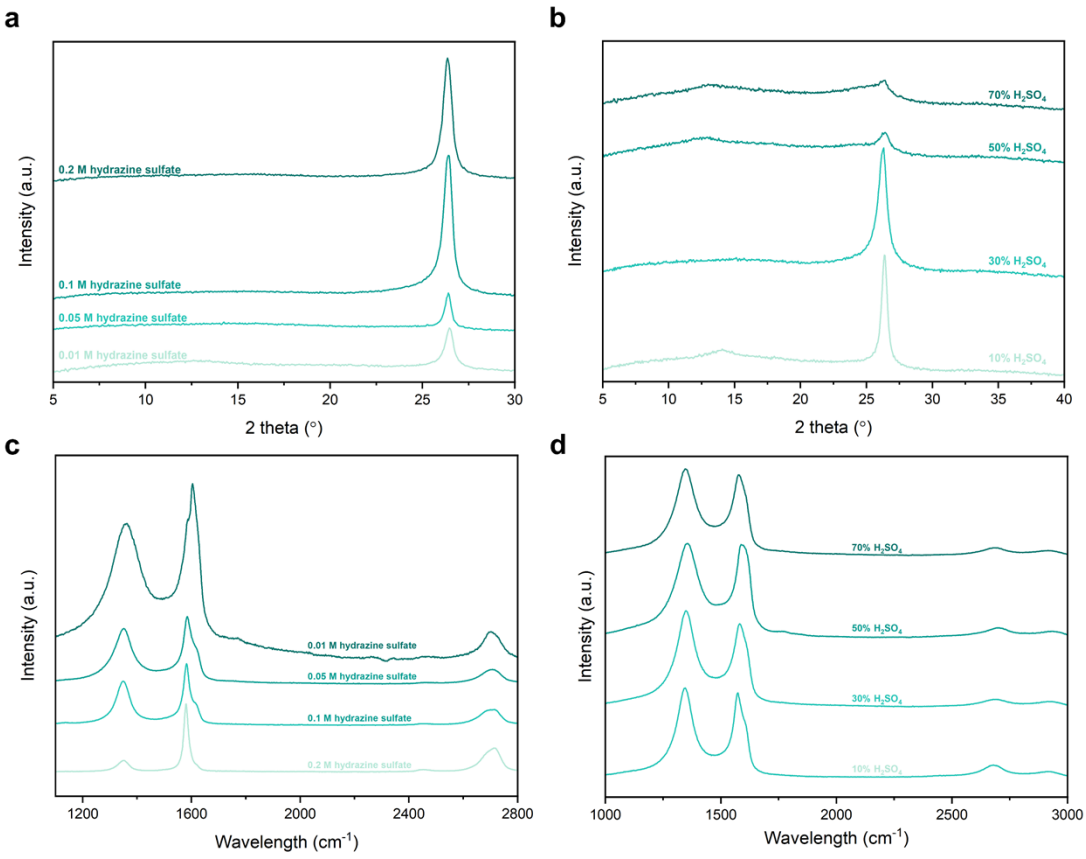

Supplementary Figure S1. Electrolyte concentration-dependent X-ray diffraction (XRD) results and Raman spectra of exfoliated graphite oxides (GOs). XRD and Raman spectra of exfoliated GOs in the secondary electrolyte of (a) hydrazine sulfate (0.01 M to 0.2 M), (b) H_2SO_4 (10 wt% to 70 wt%).

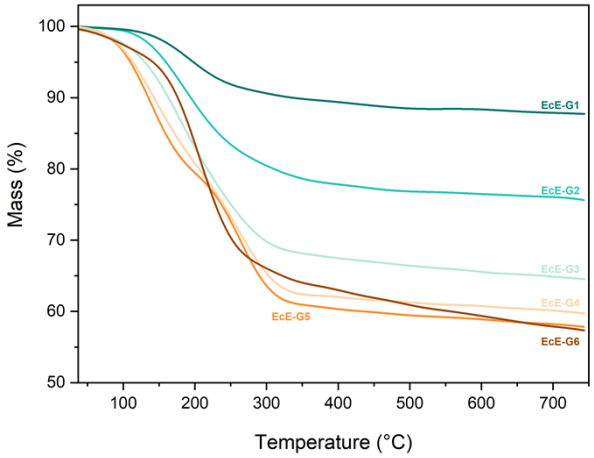

Supplementary Figure S2. The thermogravimetric analysis (TGA) of exfoliated GOs across wide oxidation degrees.

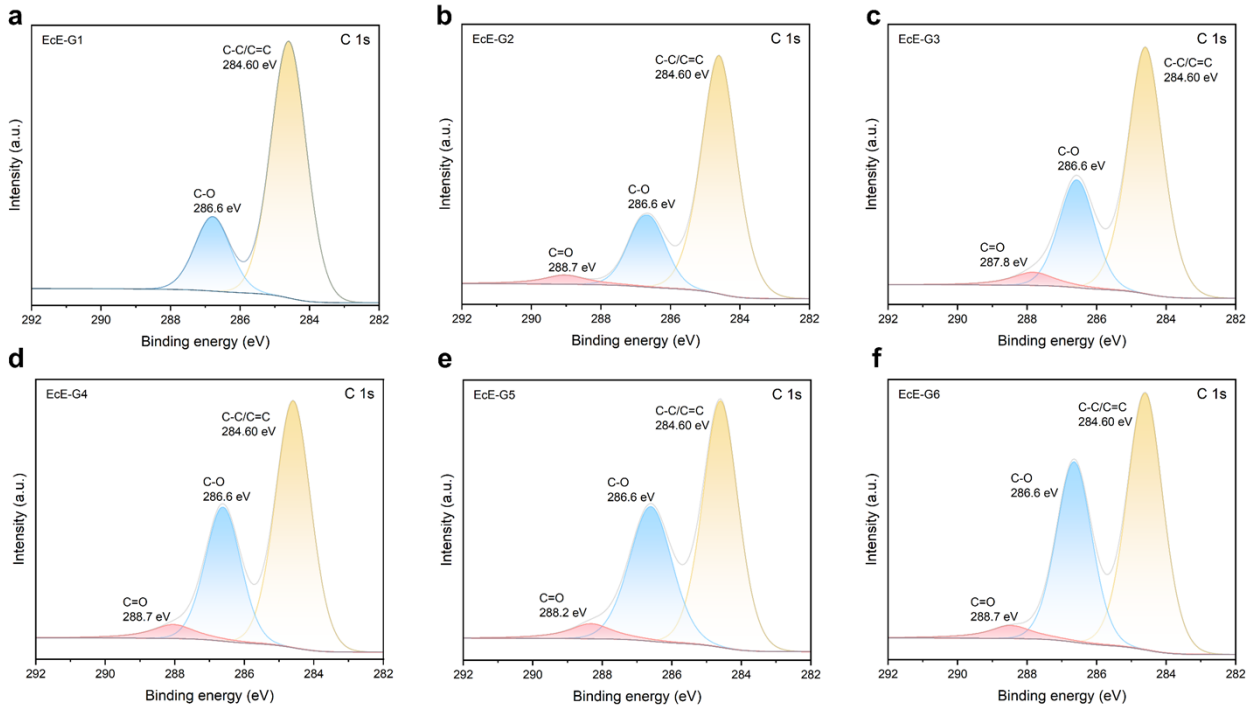

Supplementary Figure S3. The X-ray photoelectron spectroscopy (XPS) spectra for GO samples across wide oxidation degrees. Representative XPS spectra of the GOs exfoliated in post-exfoliation electrolytes include: (a) EcE-G1, (b) EcE-G2, (c) EcE-G3, (d) EcE-G4, (e) EcE-G5, and (f) EcE-G6.

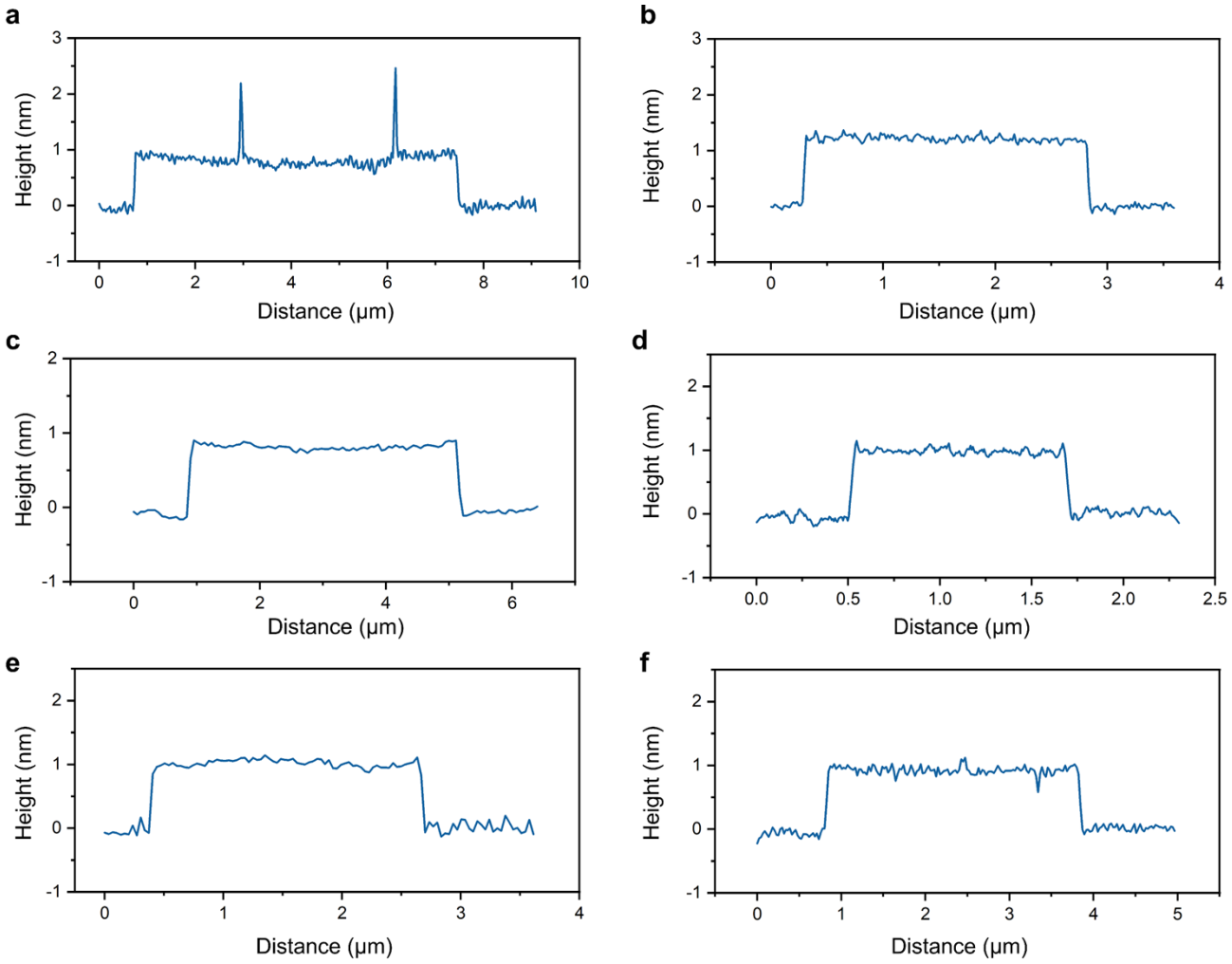

Supplementary Figure S4. The atomic force microscopy (AFM) height profiles for exfoliated GO monolayers across wide oxidation degrees. The relevant height profiles in Figure 5 (a~f) along the dashed line in each panel are presented, corresponding to (a) EcE-G1, (b) EcE-G2, (c) EcE-G3, (d) EcE-G4, (e) EcE-G5, and (f) EcE-G6.

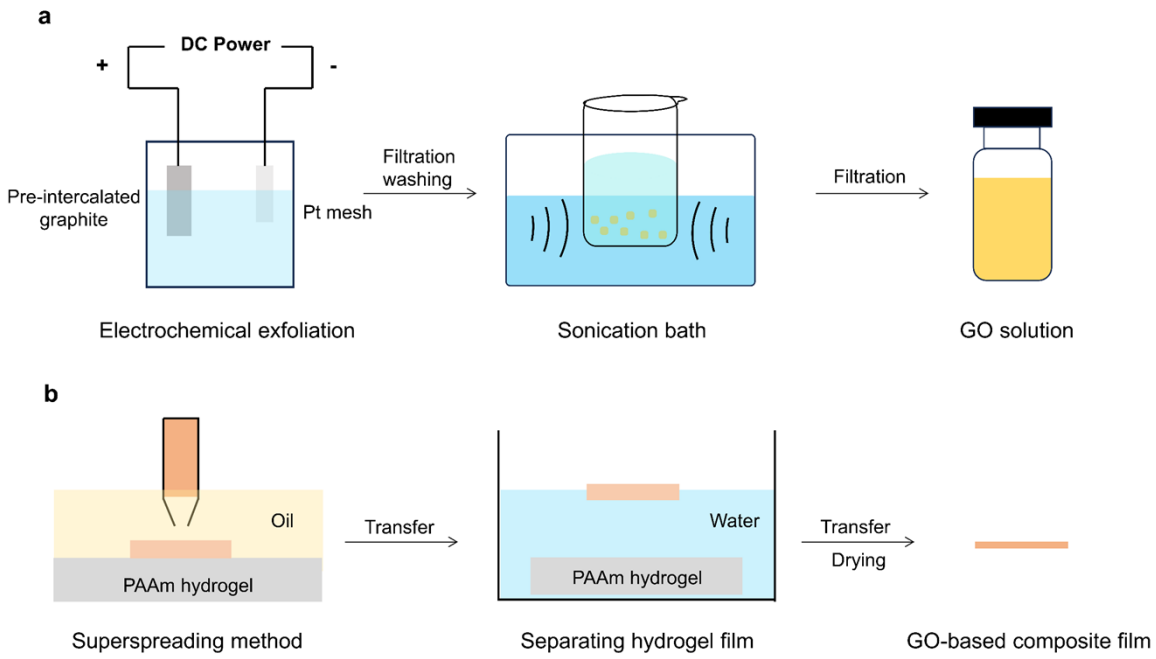

Supplementary Figure S5. The schematic illustration of the fabrication of GO-based composite films. (a) The two-step electrochemical approach for the mass production of GO nanosheets. (b) Preparation of composite films using the superspreading method.

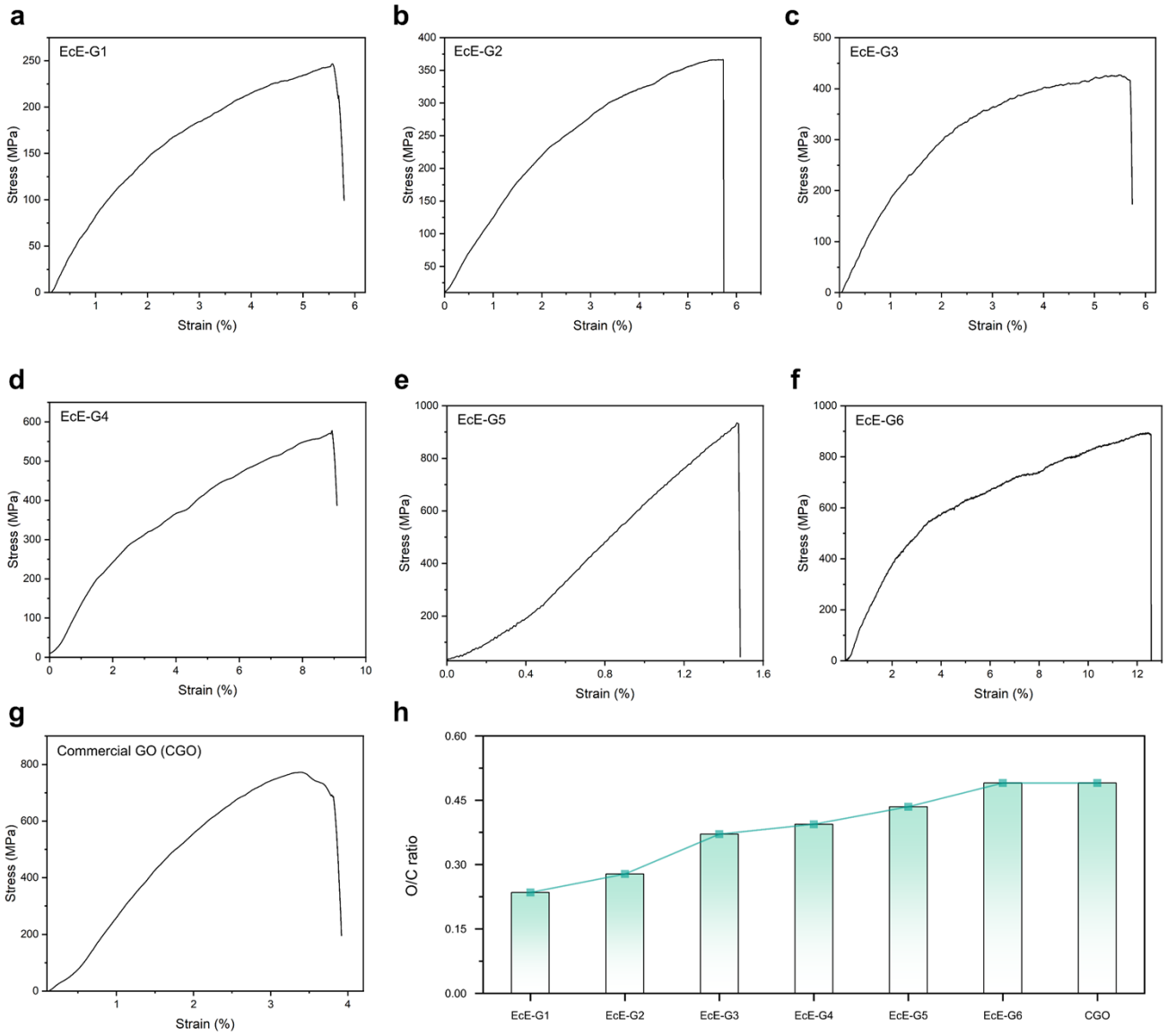

Supplementary Figure S6. The stress-strain curves for composite films composed of polymer and GO across wide range of oxidation degrees. (a) EcE-G1. (b) EcE-G2. (c) EcE-G3. (d) EcE-G4. (e) EcE-G5. (f) EcE-G6. (g) Commercial GO. (h) The elemental ratios of oxygen to carbon (O/C) of EcE-G1, EcE-G2, EcE-G3, EcE-G4, EcE-G5, EcE-G6, and commercial GO.

Table S1. The comparison of measured hole and electron mobility in field-effect transistor devices based on chemical exfoliated GO and rGO.

Types of Graphene	Number	Chemical treatment	Hole mobility ($cm^2 V^{-1} s^{-1}$)	Electron mobility ($cm^2 V^{-1} s^{-1}$)	Reference
Graphene Oxide (GO)	1	GO	0.1-1	N.A.	[1]
	2	GO	0.01-10	N.A.	[2]
Reduced Graphene Oxide (rGO)	3	Photo-reduced GO	0.03	0.01	[3]
	4	Thermal (1000 °C)-reduced GO	5.1	1.1	[4]
	5	Reduced GO	0.01-12	N.A.	[5]
	6	Hydrazine-reduced GO	0.25-0.67	N.A.	[6]
	7	Hydrazine-reduced GO	43.6	14.9	[7]
	8	Hydrazine-reduced GO	2-200	0.5-30	[8]
	9	Na-NH_3-reduced GO	123	N.A.	[9]
	10	Reduced GO	0.05-200	N.A.	[10]
	11	Hydriodic/trifluoroacetic acid-reduced GO	250	200	[11]
	12	Thermal (1000 °C)-reduced GO (multi-layer)	365	281	[4]
Liquid-phase Exfoliated Graphene (LPE-G)	13	LPE-G	95	N.A.	[12]
Electrochemical Exfoliated Graphene	14	Diluted H_2SO_4-EcE-G	5.5-17	N.A.	[1]

(EcE-G)	15	$(NH_4)_2SO_4$-EcE-G	310	N.A.	[13]
	16	Radical-assisted-EcE-G	405	N.A.	[14]
	17	Two-step Electrochemical Exfoliated Graphene	562	892	This Work

Table S2. The elemental ratios of carbon to oxygen (C/O) of various types of graphene and their respective oxidants, along with the oxidation duration.

Types of graphene	C/O ratio	Oxidant	Data source
EcE-G1	4.26	0.01 M Hydrazine sulfate	This work
EcE-G2	3.60	0.1 M Ammonium sulfate	This work
EcE-G3	2.70	50 wt% H_2SO_4 + 0.001 M $KMnO_4$	This work
EcE-G4	2.54	50 wt% H_2SO_4 + 0.0001 M $KMnO_4$	This work
EcE-G5	2.30	50 wt% H_2SO_4 + 0.01 M $KMnO_4$	This work
EcE-G6	2.04	50 wt% H_2SO_4 + 0.1 M $KMnO_4$	This work
Commercial GO	2.04	Concentrated H_2SO_4 + 3 g/g $KMnO_4$+ 5 mL/g H_2O_2	[15]
Hofmann's method GO	3.65	Concentrated H_2SO_4 + 9 mL/g HNO_3 + 11 g/g $KClO_3$	[16]
Staudenmaier's method GO	4.00	Concentrated H_2SO_4 + 9 mL/g fuming HNO_3 + 11 g/g $KClO_3$	[16]
Hummers' method GO	2.05-3.30	Concentrated H_2SO_4 +6 g/g $KMnO_4$	[17]

Reference

1. C. Su, A. Lu, Y. Xu, F. Chen, A. N. Khlobystov and L. Li, *ACS Nano*, 2011, **5**, 2332–2339.
2. K. Parvez, S. Yang, X. Feng, and K. Müllen, *Synth. Met.*, 2015, **210**, 123–132.
3. H. Li, S. Pang, S. Wu, X. Feng, K. Müllen and C. Bubeck, *J. Am. Chem. Soc.*, 2011, **133**, 9423–9429.
4. S. Wang, P. K. Ang, Z. Wang, A. L. L. Tang, J. T. L. Thong and K. P. Loh, *Nano Lett.*, 2010, **10**, 92–98.
5. K. Parvez, R. Li, S. R. Puniredd, Y. Hernandez, F. Hinkel, S.Wang, X. Feng and K. Müllen, *ACS Nano*, 2013, **7**, 3598–3606.
6. T. Kobayashi, N. Kimura, J. Chi, S. Hirata and D. Hobara, *Small*, 2010, **6**, 1210–1215.
7. J. Yang, J. W. Kim and H. S. Shin, *Adv. Mater.*, 2012, **24**, 2299–2303.
8. C. G. Navarro, R. T. Weitz, A. M. Bittner, M. Scolari, A. Mews, M. Burghard and K. Kern, *Nano Lett.*, 2007, **7**, 3499–3503.
9. H. Feng, R. Cheng, X. Zhao, X. Duan and J. Li, *Nat. Commun.*, 2013, **4**, 1539.
10. D. Joung and S. I. Khondaker, *Phys. Rev. B*, 2012, **86**, 235423.
11. S. Eigler, M. Enzelberger-Heim, S. Grimm, P. Hofmann, W. Kroener, A. Geworski, C. Dotzer, M. Röckert, J. Xiao, C. Papp, O. Lytken, H. P. Steinrück, P. Müller and A. Hirsch, *Adv. Mater.*, 2013, **25**, 3583–3587.
12. F. Torrisi, T. Hasan, W. Wu, Z. Sun, A. Lombardo, T. S. Kulmala, G. W. Hsieh, S. Jung, F. Bonaccorso, P. J. Paul, D. Chu and A. C. Ferrari, *ACS Nano*, 2012, **6**, 2992–3006.
13. K. Parvez, Z. S. Wu, R. Li, X. Liu, R. Graf, X. Feng and K. Müllenm, *J. Am. Chem. Soc.*, 2014, **136**, 6083–6091.
14. S. Yang, S. Brüller, Z. S. Wu, Z. Liu, K. Parvez, R. Dong, F. Richard, P. Samorì, X. Feng and K. Müllen, *J. Am. Chem. Soc.*, 2015, **137**, 13927–13932.
15. J. Chen, B. Yao, C. Li and G. Shi, *Carbon*, 2013, **64**, 225-229.
16. J. G. S. Moo, B. Khezri, R. D. Webster and M. Pumera, *ChemPhysChem*, 2014, **15**, 2922–2929.
17. S. Shamaila, A. K. L. Sajjad and A. Iqbal, *Chem. Eng. J.*, 2016, **294**, 458–477.